JOURNAL OF MATERIALS SCIENCE 27 (1992) 6597–6604

Optical properties of tin diselenide films

M. M. EL-NAHASS
Physics Department, Faculty of Education, Ain Shams University, Roxy, Cairo, Egypt

$SnSe_2$ films were deposited on substrates at 300 K by a conventional thermal evaporation technique. The as-deposited films were amorphous and transformed to the crystalline phase on post-deposition annealing above 573 K in an inert atmosphere. The optical properties of the films were investigated, using spectrophotometric measurements of the transmittance and reflectance at normal incidence in the wavelength range 400–2000 nm. The refractive index data fit a single oscillator model with a dispersion parameter 5.149×10^{-14} and 5.773×10^{-14} eV m^2 for the amorphous and crystalline films, respectively. The high-frequency dielectric constant of the amorphous films decreased from 9.871 to 7.475 for the crystalline films. The analysis of the spectral behaviour of the absorption coefficient in the intrinsic absorption region revealed an indirect forbidden and a direct allowed transition with energy gaps 0.99 and 2.05 eV for the amorphous films and 0.96 and 2.02 eV for the crystalline films, respectively.

1. Introduction

Tin diselenide ($SnSe_2$) has been shown to be an n-type semiconductor [1–3]. It has the CdI_2-type hexagonal structure, belonging to the D^3_{3d} symmetry group [2, 4]. The optical properties of n-type single crystals have been studied, and a broad contradiction concerning the fundamental energy gap exists. A direct transition band gap of 1.62 eV and a threshold for possible indirect phonon-assisted transitions occurring at 0.97 eV were determined from transmittance and reflectance measurements for light polarized perpendicular to the crystallographic symmetry axis of n-type single crystals of $SnSe_2$ [5]. An energy gap of 1.00 ± 0.03 eV due to a forbidden indirect transition was reported from absorption measurements [6]. The value of the energy gap, determined from the temperature dependence of the resistivity, was given as 1.0 eV [2, 3]. Further, analysis of absorption measurements indicated that the intrinsic absorption edge (at 77 K) arises from forbidden indirect transitions across energy gaps of less than or equal to 1.03 and 1.30 eV, and allowed direct transitions across an energy gap of 1.97 eV [7].

The electronic band structure of $SnSe_2$ was calculated by using an empirical pseudopotential method [8]. A direct energy gap of 1.78 eV due to a transition near the M point was obtained (the calculated transition at the M point itself is forbidden). The calculated fundamental energy gap of 0.81 eV is indirect, due to transitions between the maximum of the valence band at the Γ point and the minimum of the conduction band at the L point. Optical absorption study of single-crystal platelets of $SnSe_2$ revealed that the intrinsic absorption edge arises from a forbidden indirect transition across an energy gap of 0.98 eV and an allowed direct transition across an energy gap of 2.1 eV [9]. The band structure of $SnSe_2$, calculated by the tight-binding method, gave calculated direct and indirect gaps of 1.63 and 1.44 eV due to the $\Gamma_2^- - T_1^+$ and $\Gamma_2^- - L_1^+$ transitions, respectively [10].

In the thin film form, $SnSe_2$ has received little attention, compared to the other IV–VI compounds. The flash evaporation of stoichiometric bulk $SnSe_2$ yielded amorphous Se-rich films at substrate temperatures below 398 K [11]. Single-phase polycrystalline and stoichiometric films were deposited in the substrate temperature range 398 to 623 K. At higher substrate temperature (> 673 K) the films were non-stoichiometric and mixed phases.Thermal evaporation in a vacuum of stoichiometric bulk $SnSe_2$ resulted in amorphous films, and annealing at 423 K for 3 h resulted in recrystallization of the film [12]. A multiphase structure was detected above 573 K.

In the present work, thin films of $SnSe_2$ were deposited on substrates at room temperature, using the thermal evaporation technique in 10^{-3} Pa vacuum. The structure and optical properties of the as-deposited and post-deposition annealed films were investigated.

2. Experimental procedure

The $SnSe_2$ material was prepared by mixing stoichiometric proportions of the pure (99.999%) elements in a vacuum-sealed quartz ampoule. The sealed ampoule was placed in a furnace, the temperature of which was raised slowly until reaching 1050 K where it was then agitated for 24 h by means of an agitator attached to an electric motor. This was necessary to ensure complete mixing and reaction of the constituents. The ampoule was then cooled very slowly to 800 K and it was left at this temperature for 24 h.

Thin films were prepared from the bulk material by a conventional thermal evaporation technique on

0022–2461 © *1992 Chapman & Hall*

glass and quartz substrates using molybdenum boats. The vacuum was kept at about 10^{-3} Pa during deposition. The film thickness and the deposition rate were controlled during deposition by means of a quartz crystal thickness monitor and were also determined interferometrically [13].

The transmittance T and reflectance R of the films deposited on quartz substrates were determined at normal incidence of light in the wavelength range from 400 to 2000 nm by means of a double-beam spectrophotometer (Cary 2390, Varian) attached to a specular reflection stage with a V–W configuration.

If I_{ft} and I_q are the intensity of light passing through the film–quartz system and that through the reference quartz, respectively, then [14, 15]

$$T = \left(\frac{I_{ft}}{I_q}\right)(1 - R_q) \qquad (1)$$

where R_q is the reflectance of quartz. In addition, if the intensity of light reflected from the sample mirror reaching the detector is I_{fr} and that reflected from the reference mirror is I_m, then

$$R = \left(\frac{I_{fr}}{I_m}\right)^{1/2} - T^2 R_q \qquad (2)$$

From the measured T, R and the film thickness, the values of the refractive index n and the absorption index k were computed by a modified version [16] of the Abélès and Thèye technique [17] based on solving the two non-linear equations

$$f_t(n, k) = T_{n,k} - T_{exp.} = 0 \qquad (3)$$

$$f_r(n, k) = R_{n,k} - R_{exp.} = 0 \qquad (4)$$

where $T_{n,k}$ and $R_{n,k}$ refer to Murmann's exact equations [18, 19].

3. Results and discussion

Fig. 1 shows an X-ray diffractogram of the prepared bulk $SnSe_2$ after fine powdering. Analysis of the pattern indicated that the bulk material corresponds to a hexagonal crystal structure with lattice parameters $a = 0.381$ nm, $c = 0.61405$ nm [7]. Table I gives the observed d spacings, compared with the standard values.

Thin films deposited by thermal evaporation of the bulk material on substrates at 300 K give X-ray diffraction patterns (curve a, Fig. 2) indicating that they are amorphous. Post-deposition annealing in an inert atmosphere (argon) for 3 h led to recrystallization, beginning at an annealing temperature of 373 K. This was characterized by the appearance of the reflecting (0 0 1) basal plane of $SnSe_2$ (curve b, Fig. 2). On raising the annealing temperature, high-order reflecting planes appeared indicating the layer structure of the grown crystallites. Of course, the crystallite size increases with the annealing temperature as could be detected from the increasing abundance of the (0 0 1) basal plane. Table I compares the observed d spacing of the post-annealed films with those of the bulk $SnSe_2$.

TABLE I X-ray diffraction data of $SnSe_2$ bulk and films compared with standard data

hkl	JCPDS card 23–602		Bulk		Thin film (T_A = 573 K)	
	d(nm)	I	d(nm)	I	d(nm)	I
001	0.614	20	0.615	100	0.610	100
101	0.291	100	0.293	5	0.292	3
003	0.205	12	0.204	15	0.204	3
110	0.191	40	0.191	5		
111	0.182	12	0.183	2		
004	0.154	16	0.153	19	0.154	2
104	0.139	6	0.139	2		
114	0.119	12	0.119	4		

Since as-deposited $SnSe_2$ films on substrates at 300 K are amorphous and recrystallization occurs on post-deposition annealing, it was very interesting to investigate their optical properties. The spectral behaviour of the normal-incidence transmittance T and reflectance R for as-deposited amorphous $SnSe_2$ films and for the same films after post-deposition annealing at 573 K in an argon atmosphere for 3 h (i.e. for crystalline $SnSe_2$ films) in the wavelength range 400–2000 nm are shown in Figs 3 and 4, respectively. At long wavelengths in the transmission region $T + R = 1$, indicating that the investigated films exhibit no scattering or absorption.

The refractive and absorption indices, n and k, of $SnSe_2$ films were determined from the absolute values of the measured transmittance and reflectance at normal light incidence after correcting for the absorbance and reflectance of the substrate as given by Equations 1 and 2. The determined values were computed via Murmann's exact equations as mentioned above.

Fig. 5 shows the dispersion of the refractive index $n(\lambda)$, in the range 400 to 2000 nm for as-deposited amorphous $SnSe_2$ films and the recrystallized $SnSe_2$ films. The values shown represent the mean values

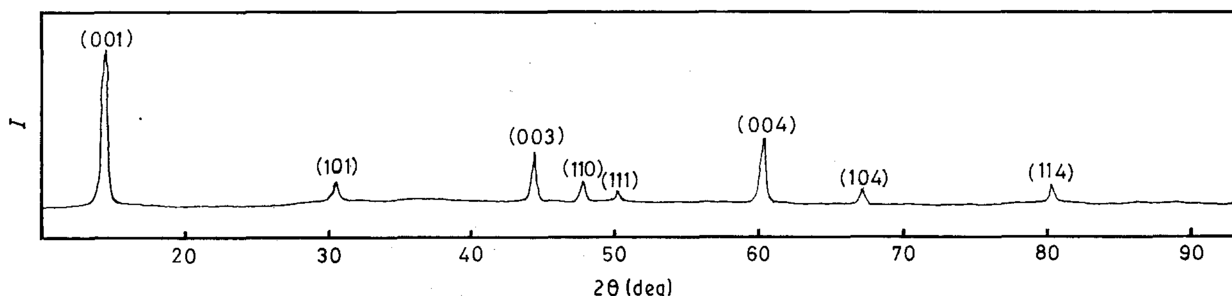

Figure 1 X-ray diffractogram of bulk $SnSe_2$.

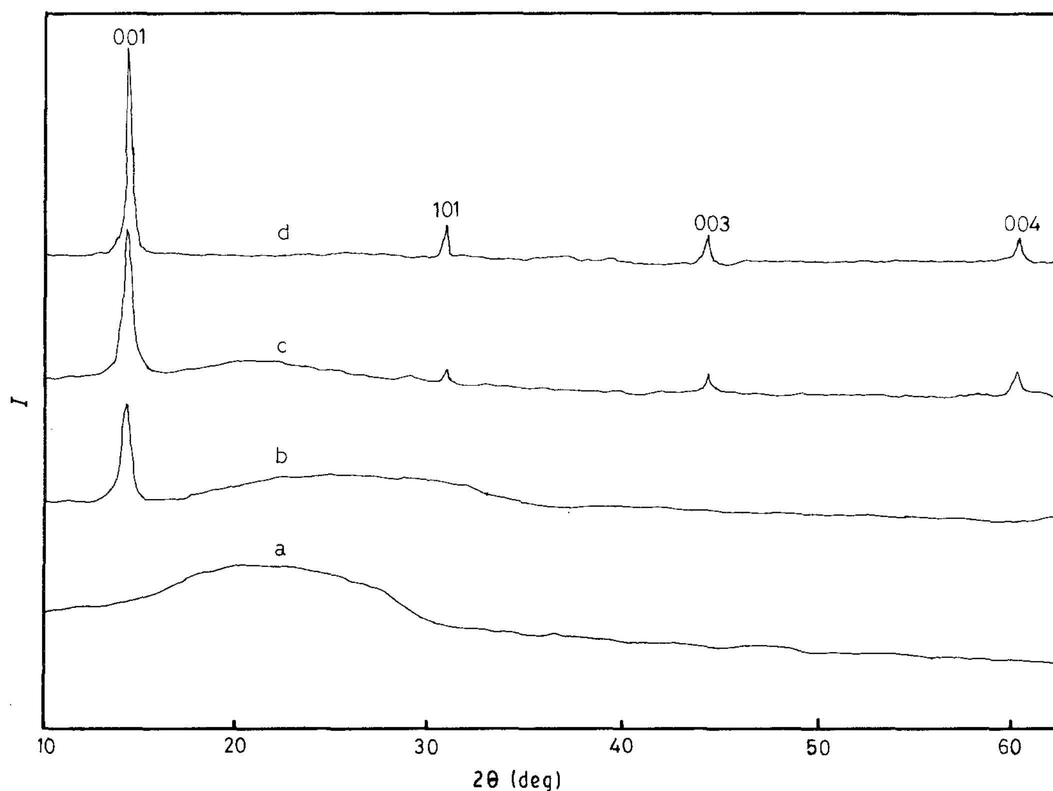

Figure 2 X-ray diffractograms of thin films of $SnSe_2$: (a) as-deposited, (b) annealed at 373 K, (c) annealed at 473 K and (d) annealed at 573 K.

Figure 3 Normal-incidence transmittance T and reflectance R of as-prepared $SnSe_2$ films. Film thickness (nm): (– · –) 70.3, (×) 93.5, (○) 135.5, (●) 194.7, (△) 270.7, (▲) 350.4.

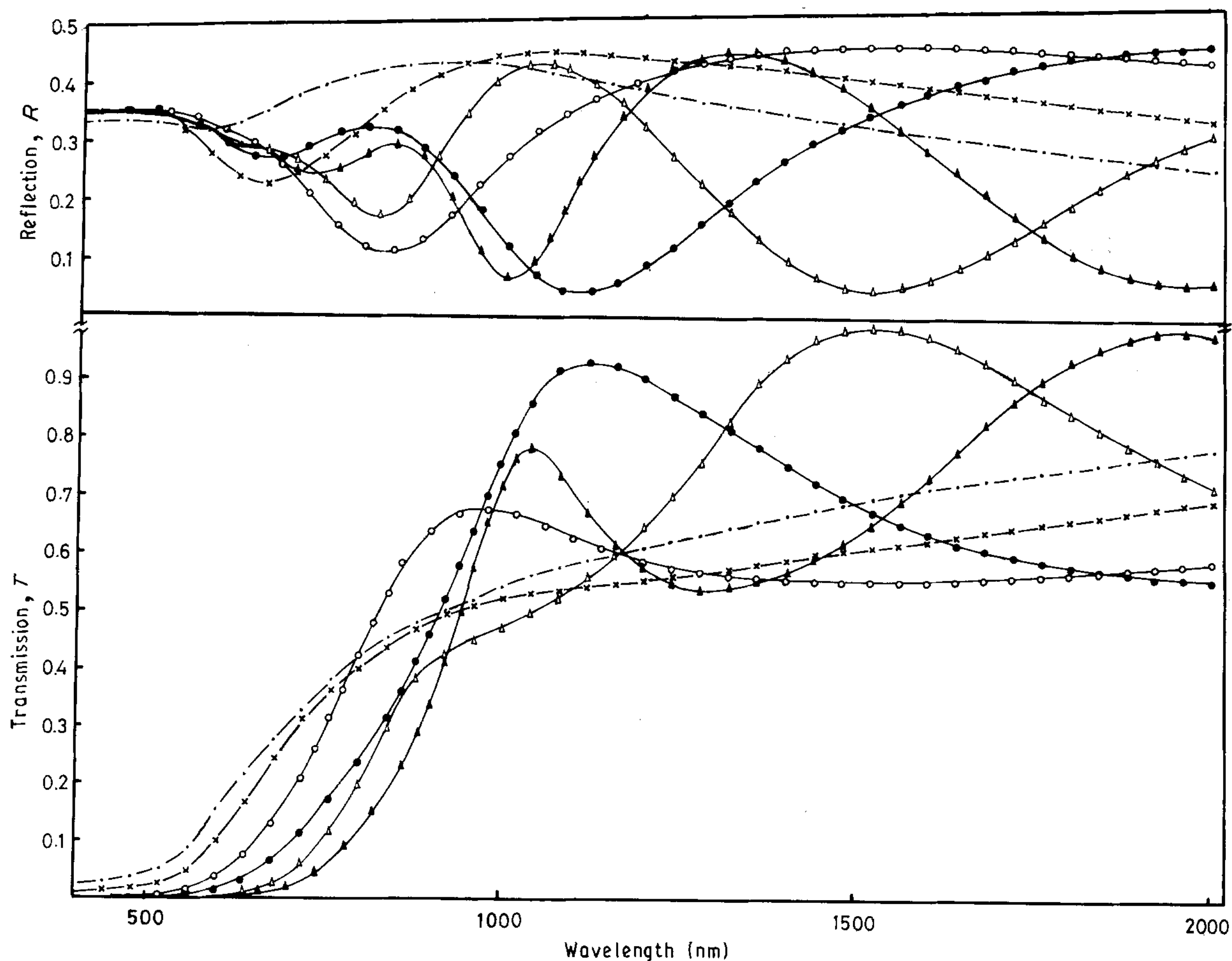

Figure 4 Normal-incidence transmittance T and reflectance R of $SnSe_2$ films after being annealed at 573 K for 3 h. Film thickness (nm): (– · –) 70.3, (×) 93.5, (○) 135.5, (●) 194.7, (△) 270.7, (▲) 350.4.

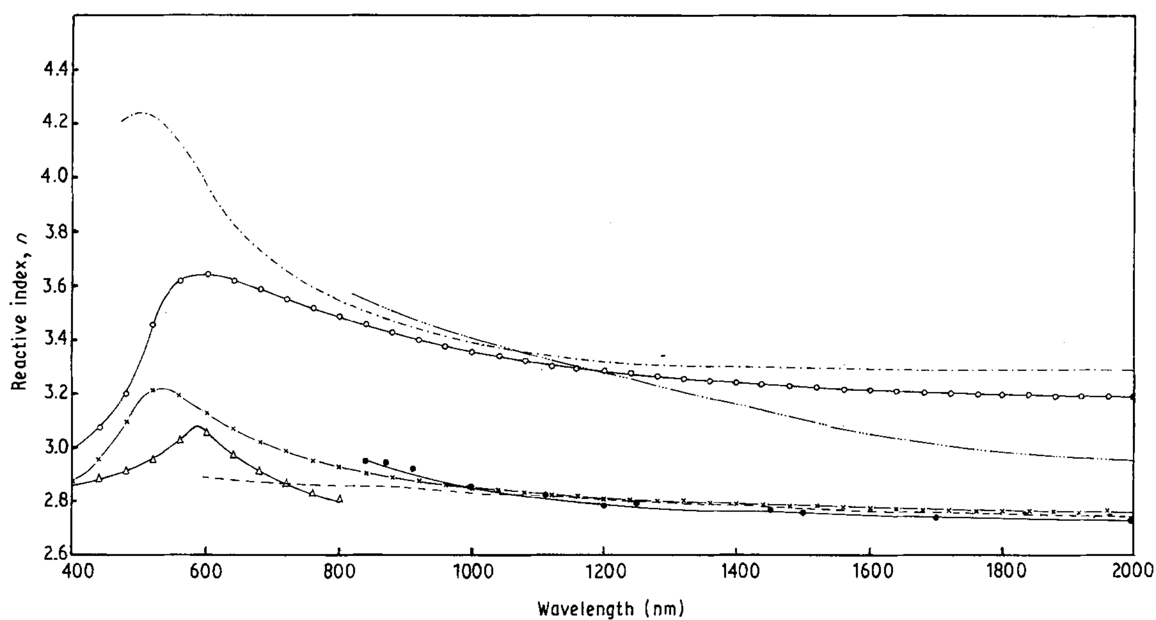

Figure 5 Dispersion of the refractive index, $n(\lambda)$, of (○) as-prepared and (×) annealed $SnSe_2$ films. Previous data are shown in the figure for comparison: (△) Kostyshin and Romonenko [20], (– – –) Domingo *et al.* [5], (●) Lee and Said [6], (– · –) Evans and Hazelwood [7], (– · · · –) Garg *et al.* [9].

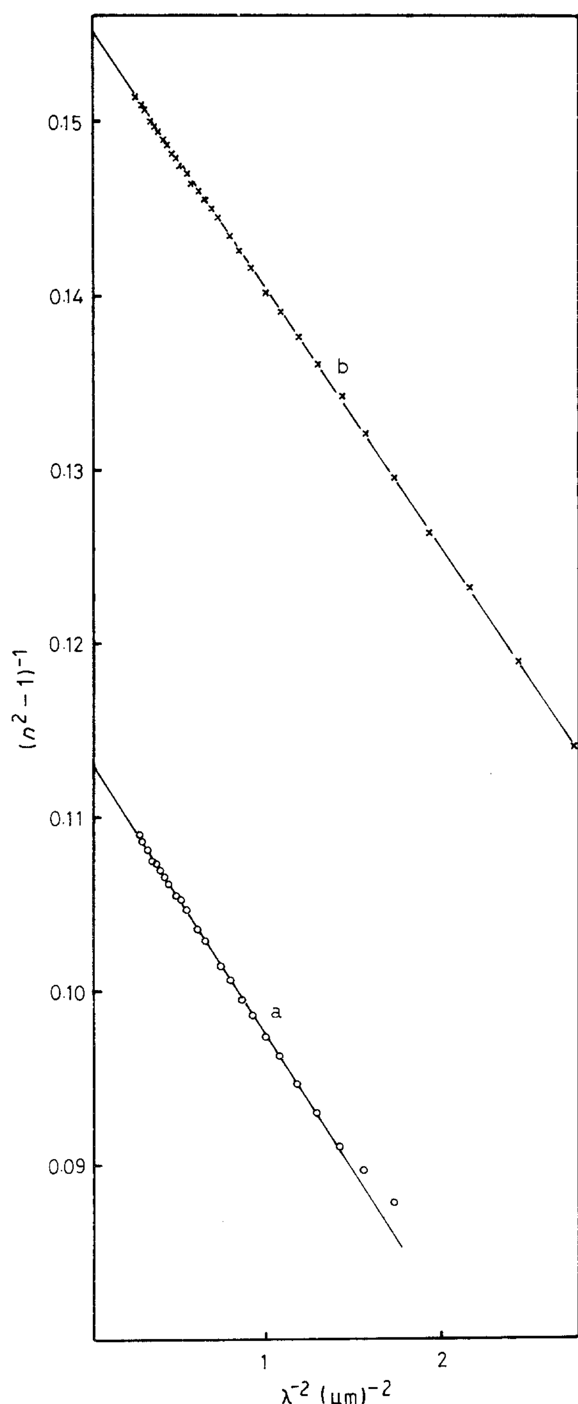

Figure 6 Plot of $(n^2 - 1)^{-1}$ versus λ^{-2} of (a) as-prepared and (b) annealed $SnSe_2$ films.

determined from films of different thickness. The refractive index data are compared with the published data in the same figure. Taking into account the experimental error in measuring the film thickness to be $\pm$ 2.5% and in T and R to be $\pm$ 1%, the error in the calculated values of n and k was estimated to be $\pm$ 2.25% and $\pm$ 2.3%, respectively.

Index of refraction data could be fitted to a single-term Sellmeir relation [21]

$$n_\lambda^2 - 1 = \frac{S_0\lambda^2}{1 - (\lambda_0/\lambda)^2} \tag{5}$$

where λ_0 is an average oscillator position and S_0 is an average oscillator strength. Plotting $1/(n^2 - 1)$ versus $1/\lambda^2$ fits a straight line at long wavelengths (Fig. 6). The experimental data deviate from the straight line at $1/\lambda^2 > 1.2$ and 2.5 μm^{-2} for the amorphous and crystalline $SnSe_2$ films, respectively. The slope of the resulting straight line gives $1/S_0$ and the infinite-wavelength intercept gives $1/S_0\lambda_0^2$. The evaluated values of S_0 and λ_0 are 0.654×10^{14} m^{-2} and 0.368 μm for the amorphous films and 0.713×10^{14} m^{-2} and 0.301 μm for the crystalline films, respectively. The dispersion parameter E/S_0, where $E = hc/e\lambda_0$ (h, c and e are the Planck constant, the speed of light and the electronic charge, respectively), is 5.149×10^{-14} and 5.773×10^{-14} eV m^2 for the amorphous and crystalline $SnSe_2$ films, respectively. Substituting the values of S_0 and λ_0 in Equation 5, a plot of refractive index versus wavelength is obtained, shown in Fig. 7 by solid lines for the amorphous and crystalline films, together with the experimental points. The good agreement between the experimentally and theoretically evaluated values in the transmission and low-absorption region shows that the single-oscillator model adequately describes the refractive index dispersion in the region considered. Hence, applying the simple classical dispersion relation [22], the refractive index varies as

$$\frac{n_\infty^2 - 1}{n^2 - 1} = 1 - \left(\frac{\lambda_0}{\lambda}\right)^2 \tag{6}$$

where n_∞ is the refractive index of an empty lattice at infinite wavelength. Extrapolating the $1/(n^2 - 1)$ versus $1/\lambda^2$ plot yields $\varepsilon_\infty = n_\infty^2$ equal to 9.871 and 7.475

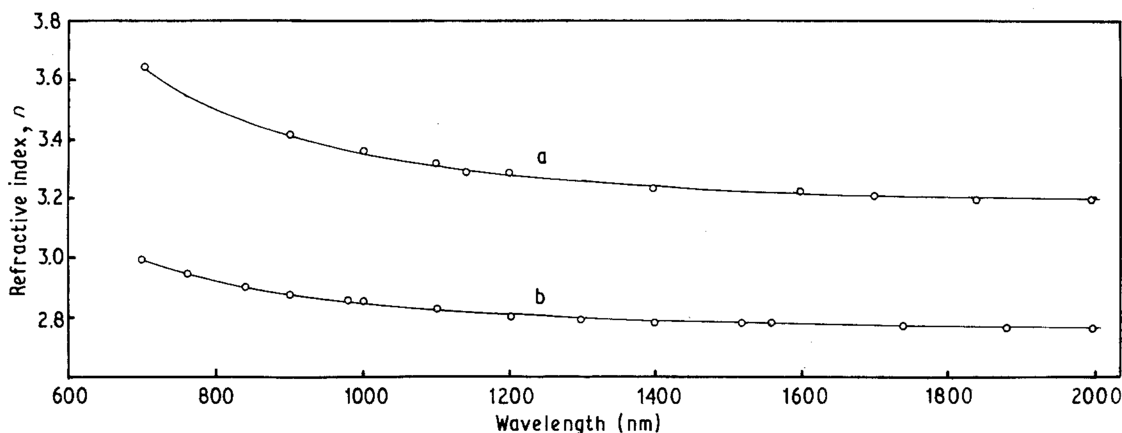

Figure 7 Plot of refractive index versus λ fitted to a single-oscillator model of (a) as-prepared and (b) annealed $SnSe_2$ films.

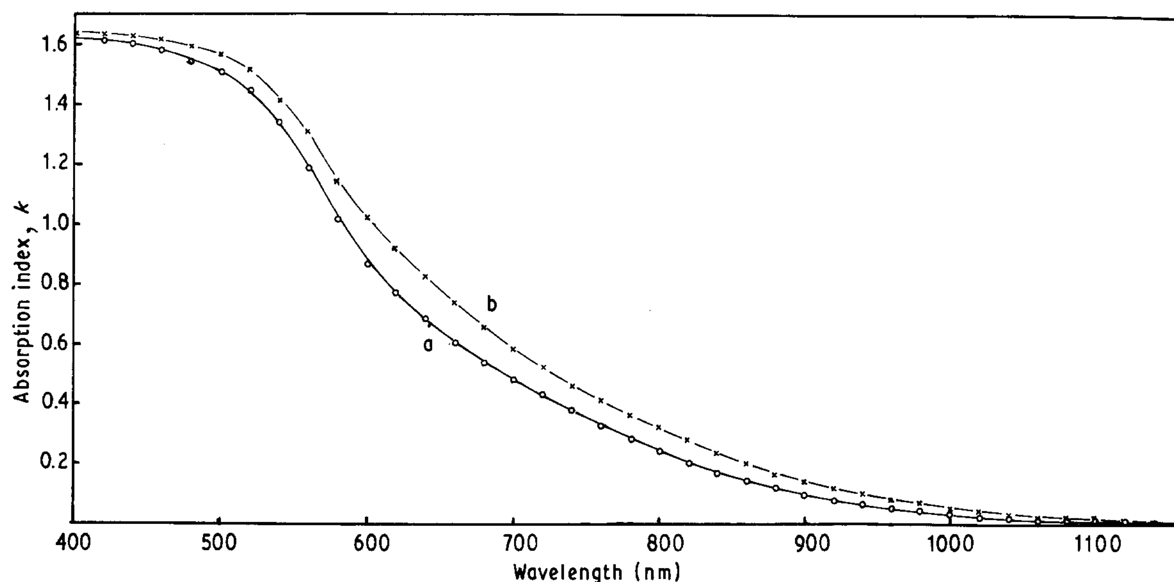

Figure 8 Spectral behaviour of the absorption index, k, of (a) as-prepared and (b) annealed $SnSe_2$ films.

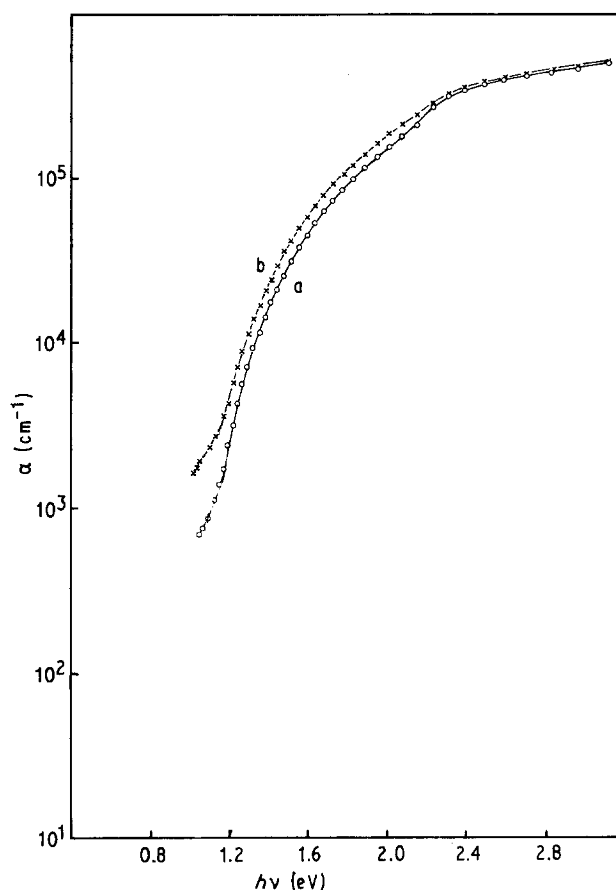

Figure 9 Spectral behaviour of the absorption coefficient α of (a) as-prepared and (b) annealed $SnSe_2$ films.

for the amorphous and crystalline $SnSe_2$ films, respectively.

Fig. (8) shows the spectral behaviour of the average values of the calculated absorption index k for the as-prepared and post-deposition annealed films at 573 K. Absorption starts near $\lambda = 1120$ nm for the as-prepared films and shifts to longer λ after annealing. The spectral behaviour of the absorption coefficient, $\alpha = 4\pi k/\lambda$, is shown in Fig. 9 for both virgin and annealed films. It is observable that the absorption edge shifts to the lower-energy side after annealing the as-prepared films at 573 K. As-deposited films were amorphous and the heat-treated films were crystalline in their structure, as shown above. The absorption

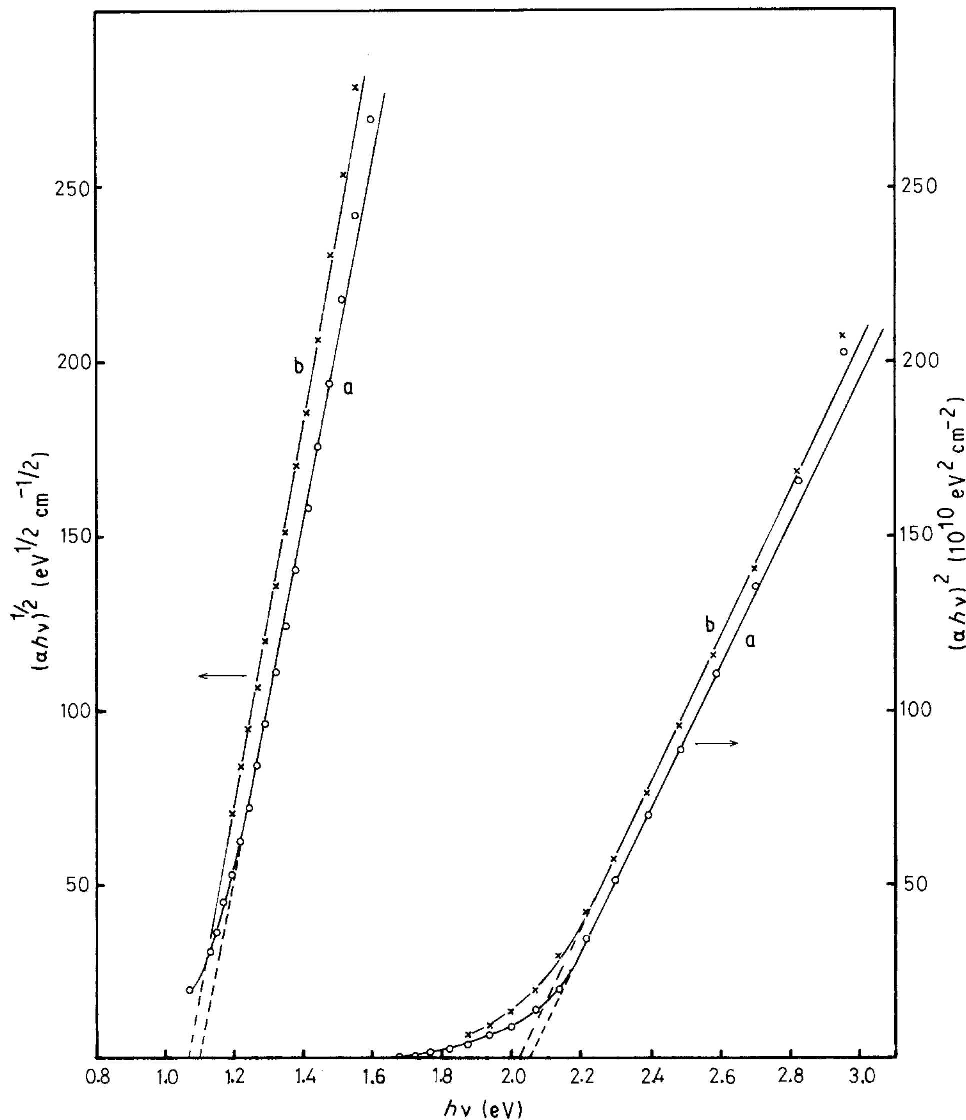

Figure 10 Plot of $(\alpha h\nu)^{1/2}$ and $(\alpha h\nu)^2$ versus $h\nu$, for (a) as-prepared and (b) annealed $SnSe_2$ films.

edge has sharpened and moved towards lower energies when the films were heat-treated. The absorption coefficient also decreased in the heat-treated films.

The intrinsic absorption edge was examined using the equation of Bardeen *et al.* [23], which states that the absorption coefficient α is given by

$$\alpha h\nu = A(h\nu - E_g)^x \tag{7}$$

where $x = 1/2$ and $3/2$ for direct allowed and forbidden transitions, respectively, and $x = 2$ and 3 for indirect allowed and forbidden transitions, respectively.

Plots of $(\alpha h\nu)^{1/2}$ versus $h\nu$ gave straight lines (Fig. 10) characteristic of indirect allowed transitions with energy gaps of 1.10 and 1.07 eV for the amorphous and crystalline films, respectively. However, the experimental points fit such plots only in a narrow range (1.2–1.5 eV). Plots of $(\alpha h\nu)^{1/3}$ versus $h\nu$ (Fig. 11) led to straight lines fitting the experimental values of the absorption coefficient in a wide photon energy range from 1.1 to 1.8 eV. This transition corresponds to an indirect forbidden transition with energy gaps 0.99 and 0.9 eV for the amorphous and crystalline $SnSe_2$ films, respectively. The lattice transition is more probable in view of energy band structure calculations [8, 10, 24, 25].

In addition, plotting $(\alpha h\nu)^2$ versus $h\nu$ in the higher energy range above the absorption edge gives straight lines (Fig. 10) characteristic of direct allowed transitions with energy gaps 2.05 and 2.02 eV for the amorphous and crystalline films, respectively. Table II compares the present data with the published work.

TABLE II Values of energy gaps for $SnSe_2$ at room temperature

Crystalline state	Indirect forbidden energy gap (eV)	Direct allowed energy gap (eV)	Reference
Amorphous	0.99	2.05	Present work
Crystalline	0.95	2.02	Present work
Single-crystal platelets	0.98	2.1	9
Single-crystal	1.03	1.97	7
	0.97		5
	1.02		6

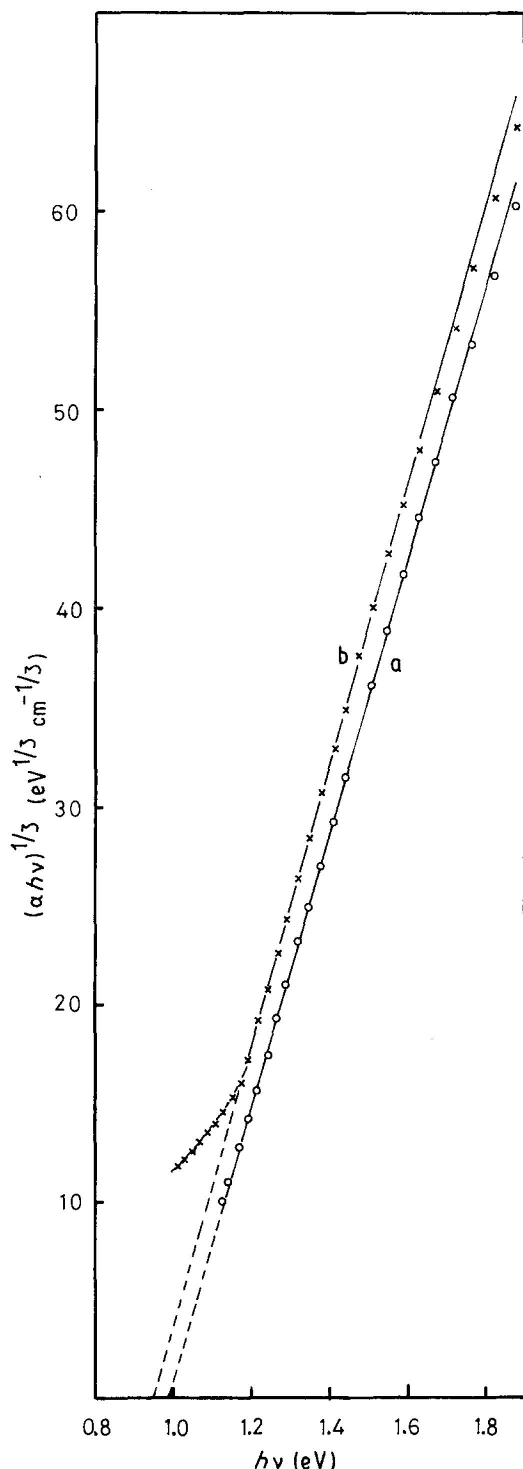

Figure 11 Plot of $(\alpha h\nu)^{1/3}$ versus $h\nu$ of (a) as-prepared and (b) annealed $SnSe_2$ films.

References

1. E. MOOSER and W. B. PERSON, *Phys. Rev.* **101** (1956) 492.
2. G. BUCH, C. FROHLICH and F. HULLIGER, *Helv. Phys. Acta* **34** (1961) 359.
3. S. ASANABE, *J. Phys. Soc. Jpn* **16** (1961) 1789.
4. R. W. G. WYCKOFF, "Crystal Structures", Vol. 1 (Interscience, New York, 1948) p. 269.
5. G. DOMINGO, R. S. ITOGA and C. R. KANNEWURF, *Phys. Rev.* **143** (1966) 536.
6. P. A. LEE and G. SAID, *Br. J. Appl. Phys. (J. Phys. D) Ser. 2* **1** (1968) 837.
7. B. L. EVANS and R. A. HAZELWOOD, *ibid*, **2** (1969) 1507.
8. M. Y. AU-YANG and M. L. COHEN, *Phys. Rev.* **178** (1969) 1279.
9. A. K. GARG, O. P. AGNIHOTRI, A. K. JAIM and R. C. TYAGI, *J. Appl. Phys.* **47** (1976) 997.
10. J. ROBERTSON, *J. Phys. C.: Solid State Phys.* **12** (1979) 4753.
11. S. M. PATEL and S. S. PATEL, *J. Mater. Sci.* **24** (1989) 3245.
12. V. P. BHATT and K. GIREESAN, *J. Mater. Sci. Lett.* **9** (1990) 362.
13. S. TOLANSKY, "Multiple-beam Interference Microscopy of Metals" (Academic, London, 1970) p. 55.
14. L. A. AGIEV and I. N. SHKLYAREVSKII, *J. Prekel. Spekt.* **76** (1978) 380.
15. I. N. SHKLYAREVESKI, T. I. KORNVEEVA and K. N. ZOZULA, *Opt. Spect.* **27** (1969) 174.
16. M. M. EL-NAHASS, H. S. SOLIMAN, N. EL-KADRY, A. Y. MORSY and S. YAGHMOUR, *J. Mater. Sci. Lett.* **7** (1988) 1050.
17. F. ABÉLÈS and M. L. THEYÈ, *Surf. Sci.* **5** (1966) 325.
18. O. S. HEAVENS, in "Physics of Thin Films", Vol. 2, (edited by G. Hass and R. Thus (Academic, New York, 1964) p. 193.
19. H. M. LIDDELL, "Computer-aided Techniques for the Design of Multilayer Filters", (Hilger, Bristol, 1981) p. 118.
20. M. T. KOSTYSHIN and P. F. ROMONENKO, *Opt. Spectroscopy*, **12** (1962) 349.
21. M. DIDOMENICO and S. H. WEMPLE, *J. Appl. Phys.* **40** (1969) 720.
22. T. S. MOSS, G. J. BURRELL and B. ELLIS, "Semiconductor Optoelectronics" (Butterworths, London, 1973) p. 23.
23. J. BARDEEN, F. J. BLATT and L. H. HALL, in Proceedings of Photoconductivity Conference, edited by R. Breckenridge, B. Russel and T. Hahn (Wiley, New York, 1956).
24. C. RAISIN, Y. BERTRAND and J. ROBIN, *Solid State Commun.* **24** (1977) 353.
25. Y. BERTRAND, A. DIVERCHY and C. RAISIN, *J. Phys. C: Solid State Phys.* **10** (1977) 4155.

Received 22 July 1991
and accepted 11 March 1992